







ISSN: 2617-6548

URL: www.ijirss.com



Optimal tracking control using discrete disturbance observer for unmanned surface vessel under unknown disturbances

 Cao Xuan Canh^{1*},  Nguyen Thi Anh¹,  Doan Van Toi¹,  Nguyen Danh Nam¹

¹*Viettel High Technology Industries Corporation, Hanoi, Vietnam.*

Corresponding author: Cao Xuan Canh (Email: canhcx@viettel.com.vn)

Abstract

This article proposes an optimal control approach to address the trajectory tracking problem for unmanned surface vessels (USVs) subjected to external disturbances such as wind, waves, and currents. An optimal control method based on the Online Adaptive Dynamic Programming (OADP) algorithm is introduced to minimize energy consumption and enhance the USV's tracking performance. A disturbance observer is employed to estimate and compensate for external disturbances effectively. The OADP algorithm incorporates a neural network layer, which simplifies the structure and improves computational efficiency. Stability analysis is conducted using Lyapunov theory, considering weights and tracking errors. Simulation results demonstrate the effectiveness of the proposed control scheme, showing improvements over sliding mode control (SMC) and online actor-critic (AC) algorithms in trajectory tracking and cost optimization under various environmental conditions.

Keywords: Discrete disturbance observer, Online Adaptive Dynamic Programming, Optimal control, Unmanned surface vessel.

DOI: 10.53894/ijirss.v8i7.10405

Funding: This study received no specific financial support.

History: Received: 11 August 2025 / Revised: 15 September 2025 / Accepted: 17 September 2025 / Published: 1 October 2025

Copyright: © 2025 by the authors. This article is an open access article distributed under the terms and conditions of the Creative Commons Attribution (CC BY) license (<https://creativecommons.org/licenses/by/4.0/>).

Competing Interests: The authors declare that they have no competing interests.

Authors' Contributions: All authors contributed equally to the conception and design of the study. All authors have read and agreed to the published version of the manuscript.

Transparency: The authors confirm that the manuscript is an honest, accurate, and transparent account of the study; that no vital features of the study have been omitted; and that any discrepancies from the study as planned have been explained. This study followed all ethical practices during writing.

Acknowledgments: The authors sincerely appreciate the support and valuable resources provided by the Modeling and Simulation Center, a division of Viettel High Technology Industries Corporation, during this study. Additionally, we deeply acknowledge the leadership team, and team members at the Modeling and Simulation Center for their dedicated assistance, insightful feedback, and significant contributions to the testing and refinement of the solution examined in this project.

Publisher: Innovative Research Publishing

1. Introduction

Unmanned surface vessels (USV) have gotten the attention of researchers and scientists because of their applications in transportation, military and climate, environment monitoring [1]. Trajectory tracking is a fundamental problem in control theory, especially in applications like USVs, because these systems must follow a predefined path accurately while being

unaffected with disturbances and uncertainties. Several reasons make trajectory tracking a crucial topic in control, such as autonomous navigation: the USVs often operate in complex environments where they must follow a designated path to complete tasks such as surveillance, delivery, or search and rescue, and marine surveys require precise movement along a desired path, which makes this problem always challenging [2]. Numerous algorithm developments have occurred to control it autonomously, requiring as little human intervention as possible. The model of the USV is often linearized around the operating point to implement the linear control algorithm such as proportional – integral – derivative (PID) [3] or the linear quadratic regulator (LQR) [4] however, this approach is not fully reliable because of the error in linearizing, especially when the reference trajectory represents a curve in the workspace, because the curve trajectory emphasizes the nonlinearity of the vessel motion. For those reasons, the nonlinear methods are implemented to avoid these drawbacks, one of the most popular methods is nonlinear Lyapunov - based techniques [5, 6]. However, in these works, the velocity of the yaw variable is required to be nonzero; under this restriction, straight trajectories cannot be guaranteed. Also, the drag force model, the rigid body resistance as it moves through the water is assumed to be a linear function concerning the velocity in all three DOF motions, meaning that the results are valid if only the vessel moves at low speed. The article [7] solves this restrictive assumption. One of the famous variations of Lyapunov's method is Lyapunov-based backstepping for an output feedback tracking control [8]. The sliding mode controller also becomes the mainstream solution for the model uncertainties thanks to the insensitivity [9].

Nevertheless, all of these controllers only focus on bringing the state error to zero, not taking into account the energy expended by the actuator or the value of the control signal. To tackle this problem, the model predictive control is derived as an optimal controller to minimize both state errors and the control input in a finite step of time [10]. An approach that can minimize the cost function of in overall time is the dynamic programming of Richard Bellman [11]. From a mathematical perspective, solving the optimal control problem relies on finding a solution to the Hamilton–Jacobi–Bellman (HJB) equation. However, due to the equation's strong nonlinearity, only certain solutions have been obtained. As a result, significant efforts have been made to develop algorithms that provide approximate solutions to this equation. Based on that idea, the reinforcement learning algorithm is provided, in which the cost function and optimal control input are approximated by neural networks [12].

Besides the optimization problem, the robustness with disturbances is also a challenge that is still being researched, because in practice, the appearance of disturbances affecting the USV is inevitable, such as the friction of the water, or the flow of the wind, etc. A popular approach to rejecting the influence of the disturbances is build a disturbance observer to estimate and then compensate the disturbances in the control input using a feedforward controller or indirectly suppress the impact of the disturbances through controller [13]. Another way to approach is to apply control techniques such as Lyapunov theory [14] H^∞ norm minimization [15], or integral sliding mode controller [16, 17]. In literature, disturbances are often divided into lumped disturbances [18] input disturbances [19, 20] and matched and unmatched disturbances [21, 22]. Between those types of disturbances, unmatched ones are commonly the hardest to estimate. Several disturbance estimators are introduced to observe and approximate these kinds of disturbances [23, 24]. In Trinh, et al. [25] a nonlinear disturbance observer is used to estimate the low-varying disturbances, the restriction of this observer is that the first disturbance is required to be approximately zero, which makes it impractical when applied to a real-life environment. Furthermore, certain disturbance observers require knowledge of all first derivatives of the system's states to estimate disturbances, necessitating additional sensors or more complex computations. Additionally, these observers were primarily developed for nonlinear autonomous systems. Lastly, for these observers to estimate disturbances effectively or for controllers to handle them, the disturbance and its first and higher-order derivatives must be bounded [26].

In this article, the robust optimal control based on online adaptive dynamic programming [12] is used with just one neural network to show the efficient computation and energy over the conventional 2-layered method, also, a disturbance observer is proposed to avoid the impact of the external and unknown disturbances without boundness requirement.

The rest of the paper is structured as follows: Section 2 introduces the mathematical model of the USV, in Section 3, the control design and disturbance estimation are given, and numerical simulation results are provided in Section 4. Finally, Section 5 concludes and outlines directions for future works.

2. USV Model

In this section, the model of each surface vehicle is established with 3 degrees of freedom while neglecting motion in the roll, heave and pitch axes [27]. The kinematic model is provided as follows:

$$\dot{\eta} = J(\eta)\vartheta \quad (1)$$

With

$$J(\eta) = \begin{bmatrix} \cos \psi & -\sin \psi & 0 \\ \sin \psi & \cos \psi & 0 \\ 0 & 0 & 1 \end{bmatrix} \quad (2)$$

where $\eta = [x, y, \psi]^T \in \mathbb{R}^3$ denotes the position and orientation of USV in the inertial reference frame. $\vartheta = [u, v, r]^T \in \mathbb{R}^3$ denotes the velocity of USV in the body-fixed frame. $J(\eta)$ denotes the rotation matrix.

The dynamic model is presented by the following equation, assuming the vector of gravitation and buoyancy is equal to zero:

$$M\dot{\vartheta} + C(\vartheta)\vartheta + D(\vartheta)\vartheta = \tau + \tau_d \quad (3)$$

With

$$M = \begin{bmatrix} m - X_{\dot{u}} & 0 & 0 \\ 0 & m - Y_{\dot{v}} & mx_g - Y_{\dot{r}} \\ 0 & mx_g - N_{\dot{v}} & I_z - N_{\dot{r}} \end{bmatrix} \quad (4)$$

$$C(v) = \begin{bmatrix} 0 & 0 & -M_{22}v - M_{23}r \\ 0 & 0 & M_{11}u \\ M_{22}v + M_{23}r & -M_{11}u & 0 \end{bmatrix} \quad (5)$$

$$D(v) = \begin{bmatrix} d_{11} & 0 & 0 \\ 0 & d_{22} & d_{23} \\ 0 & d_{32} & d_{33} \end{bmatrix} \quad (6)$$

where $d_{11} = -X_u - X_{uu}|u| - X_{uuu}u^2$, $d_{22} = -Y_v - Y_{vv}|v| - Y_{rv}|r|$, $d_{23} = -Y_r - Y_{vr}|v| - Y_{rr}|r|$, $d_{32} = -N_v - N_{vv}|v| - N_{rv}|r|$, $d_{33} = -N_r - N_{vr}|v| - N_{rr}|r|$. m and I_z are the mass and the moment of inertia of USV. x_g is the distance from geometric center to the center of mass of the USV.

$X_{\dot{u}}, Y_{\dot{v}}, Y_{\dot{r}}, N_{\dot{v}}, N_{\dot{r}}, X_u, X_{uu}, X_{uuu}, Y_v, Y_{vv}, Y_{vr}, Y_r, Y_{rv}, Y_{rr}, N_v, N_{vr}, N_{vv}, N_r, N_{rv}, N_{rr}$ are hydrodynamic parameters of USV. $\tau = [\tau_1, \tau_2, \tau_3]^T \in \mathbb{R}^3$ denotes the surge force, sway force and yaw moment that control the USV. $\tau_d = [\tau_{d1}, \tau_{d2}, \tau_{d3}]^T \in \mathbb{R}^3$, represents the external and unknown disturbances acting on the USV. $M \in \mathbb{R}^{3 \times 3}$, $C(\vartheta) \in \mathbb{R}^{3 \times 3}$, $D(\vartheta) \in \mathbb{R}^{3 \times 3}$ denote the inertia matrix including added mass, the Coriolis and centripetal matrix, and the hydrodynamic damping matrix.

Property 1. M is positive, that is $z^T M z > 0, \forall z \in \{\mathbb{R}^3 | z \neq [0, 0, 0]^T\}$

Property 2. $C(\vartheta)$ is skew-symmetric, that is $C(\vartheta) = C^T(\vartheta)$ and $z^T C(\vartheta) z = 0, \forall z \in \mathbb{R}^3$

Property 3. $D(\vartheta)$ is positive, that is $z^T D(\vartheta) z = \left(\frac{1}{2}\right) z^T (D^T(\vartheta) + D(\vartheta)) z > 0, \forall z \in \{\mathbb{R}^3 | z \neq [0, 0, 0]^T\}$

Property 4. $J(\eta)$ is non-singular, satisfying $J^{-1}(\eta) = J^T(\eta)$

To track the reference trajectory in the earth-fixed frame and establish the sliding variable, the dynamic model needs to be transformed with respect to the variable η . From kinematic model (2) and Property 4, having:

$$\dot{\vartheta} = J^T(\eta) \dot{\eta} \quad (7)$$

Take the time derivative of both sides of (7):

$$\dot{\vartheta} = J^T(\eta) \ddot{\eta} + \frac{\partial J^T(\eta)}{\partial t} \dot{\eta} \quad (8)$$

Define

$$S(\eta, \dot{\eta}) = \frac{\partial J^T(\eta)}{\partial t} = \begin{bmatrix} -\sin \psi & \cos \psi & 0 \\ -\cos \psi & -\sin \psi & 0 \\ 0 & 0 & 0 \end{bmatrix} \dot{\psi}$$

Eq. (8) becomes:

$$\dot{\vartheta} = J^T(\eta) \ddot{\eta} + S(\eta, \dot{\eta}) \dot{\eta} \quad (9)$$

Substituting Eq. (9) into Eq. (3):

$$M(J^T(\eta) \ddot{\eta} + S(\eta, \dot{\eta}) \dot{\eta}) + C(\vartheta) J^T(\eta) \dot{\eta} + D(\vartheta) J^T(\eta) \dot{\eta} = \tau + \tau_d \quad (10)$$

Simplify that:

$$M_{\eta}(\eta) = M J^T(\eta) \quad (11)$$

$$C_{\eta}(\eta, \vartheta) = M S(\eta, \dot{\eta}) + C(\vartheta) J^T(\eta) + D(\vartheta) J^T(\eta) \quad (12)$$

The dynamic model can be rewritten:

$$M_{\eta}(\eta) \ddot{\eta} + C_{\eta}(\eta, \vartheta) \dot{\eta} + D_{\eta}(\eta, \vartheta) \dot{\eta} = \tau + \tau_d \quad (13)$$

The sliding variable s is defined as:

$$s = \dot{e} + \Lambda e \quad (14)$$

where $\Lambda \in \mathbb{R}^{3 \times 3}$ is a diagonal positive matrix, $e = \eta_d - \eta$ is the tracking error in the inertial reference frame, $\eta_d = [x_d, y_d, \psi_d]^T$ denotes the desired trajectory that the USV needs to track.

From (14), $\ddot{\eta}$ and $\dot{\eta}$ can be written as:

$$\dot{\eta} = \dot{\eta}_d + \Lambda e - s \quad (15)$$

$$\ddot{\eta} = \ddot{\eta}_d + \Lambda \dot{e} - \dot{s} \quad (16)$$

Substituting Eqs. (15)-(16) into Eq. (13):

$$M_{\eta}(\eta)(\ddot{\eta}_d + \Lambda \dot{e} - \dot{s}) + C_{\eta}(\eta, \vartheta)(\dot{\eta}_d + \Lambda e - s) = \tau + \tau_d \quad (17)$$

We have the dynamic equation with respect to s as follows:

$$\dot{s} = -M_{\eta}^{-1}(\eta) C_{\eta}(\eta, \vartheta) s - M_{\eta}^{-1}(\eta) \tau + \ddot{\eta}_d + \Lambda \dot{e} + M_{\eta}^{-1}(\eta) C_{\eta}(\eta, \vartheta)(\dot{\eta}_d + \Lambda e) - M_{\eta}^{-1}(\eta) \tau_d \quad (18)$$

Define

$$g_{\tau} = -M_{\eta}^{-1}(\eta) \quad (19)$$

$$g_d = -M_{\eta}^{-1}(\eta) \quad (20)$$

$$f(s) = -M_{\eta}^{-1}(\eta) C_{\eta}(\eta, \vartheta) s \quad (21)$$

$$F = \ddot{\eta}_d + \Lambda \dot{e} + M_{\eta}^{-1}(\eta) C_{\eta}(\eta, \vartheta)(\dot{\eta}_d + \Lambda e) \quad (22)$$

The control-affine model can be written as the following:

$$\dot{s} = f(s) + g_\tau \tau + F + g_d \tau_d \quad (23)$$

3. Optimal Control Design for USV

Because of unmatched disturbances, the proposed controller has two parts: optimal control signal and disturbance compensation signal. The block diagram of control model is shown in Figure 1.

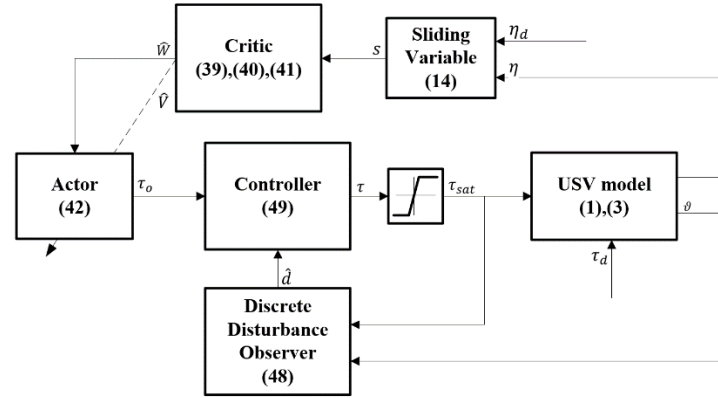


Figure 1.
Diagram of the proposed scheme.

3.1. Optimal Control Design

Assume the disturbance $\tau_d = [0 \ 0 \ 0]^T$ and omit the component F the control-affine model (23) becomes:

$$\dot{s} = f(s) + g_\tau \tau \quad (24)$$

Assumption 1. $f(s)$ is Lipschitz continuous on the set $\Omega \in \mathbb{R}^3$, containing the origin, and there exists a continuous control function $\tau(t) \in U$ such that the closed-loop system is asymptotically on Ω .

Define the optimal cost index:

$$V^*(s) = \min_{\tau \in U} \int_t^\infty r(s(t)\tau(x(t))) dt \quad (25)$$

with cost function $r(s, \tau) = s^T Q s + \tau^T R \tau$, where $Q \in \mathbb{R}^{3 \times 3}$, $R \in \mathbb{R}^{3 \times 3}$ are symmetric positive matrices.

Define the optimal Hamiltonian function:

$$H(s, \tau, V_s^*) = \left(\frac{\partial V^*}{\partial s} \right)^T \dot{s} + s^T Q s + \tau^T R \tau \quad (26)$$

The optimal control signal is calculated by the following:

$$\tau^* = \arg \min_{\tau \in U} H(s, \tau, V_s^*) \quad (27)$$

Solve the Equation 27, the optimal control signal is written:

$$\tau^* = -\frac{1}{2} R^{-1} g_\tau^T \frac{\partial V^*}{\partial s} \quad (28)$$

Substituting (24), (28) into (26), the optimal Hamiltonian function becomes:

$$s^T Q s + V_s^{*T} f(s) - \frac{1}{4} V_s^{*T} g_\tau R^{-1} g_\tau^T V_s^* = 0 \quad (29)$$

$V^*(s)$ is called the HJB solution. However, finding the solution $V^*(s)$ from the nonlinear differential equation is impossible. Therefore, $V^*(s)$ is approximated by a neural network:

$$V^*(s) = W^T \Phi(s) + \epsilon(s) \quad (30)$$

where $W \in \mathbb{R}^n$ denotes the weight component of the neural network, $\Phi(s) \in \mathbb{R}^n$ denotes the activation function, composed by basic functions of s . $\epsilon(s)$ denotes the error in approximating the optimal cost index using the neural network.

Substituting Equation 30 into Hamiltonian function:

$$H(s, \tau, W) = W^T \Phi_s (f(s) + g_\tau \tau) + s^T Q s + \tau^T R \tau - \epsilon_H = 0 \quad (31)$$

where $\Phi_s = \partial \Phi / \partial s \in \mathbb{R}^{n \times 3}$, $\epsilon_H = -\epsilon(s)(f(s) + g_\tau \tau)$

Substituting Eq. (30) into Eq. (29):

$$s^T Q s + W^T \Phi_s (f(s)) - \frac{1}{4} \Phi_s^T W G W^T \Phi_s + \epsilon_{HJB} = 0 \quad (32)$$

where $G = g_\tau R^{-1} g_\tau^T$ and

$$\epsilon_{HJB} = \epsilon_s^T f(s) - \frac{1}{2} \Phi_s^T W G \epsilon_s - \frac{1}{4} \epsilon_s^T G \epsilon_s \quad (33)$$

Transform ϵ_{HJB} :

$$\epsilon_{HJB} = \epsilon_s^T f(s) - \frac{1}{2} (\Phi_s^T W G + \epsilon_s^T G) \epsilon_s + \frac{1}{4} \epsilon_s^T G \epsilon_s$$

$$\begin{aligned}
 &= \epsilon_s^T f(s) - \frac{1}{2} (\Phi_s^T W + \epsilon_s^T) g_\tau R^{-1} g_\tau^T \epsilon_s + \frac{1}{4} \epsilon_s^T G \epsilon_s \\
 &= \epsilon_s^T (f(s) + g_\tau \tau^*) + \frac{1}{4} \epsilon_s^T G \epsilon_s
 \end{aligned} \tag{34}$$

According to Weierstrass approximation theorem, when $n \rightarrow \infty$, ϵ_{HJB} converges to 0.

However, due to the limitation of the practical computation, the number of elements of the activation function is finite, therefore the optimal cost index is approximated:

$$\hat{V}(s) = \hat{W}^T \Phi(s) \tag{35}$$

with $\hat{W} \in \mathbf{R}^n$ is the estimated weight component.

Define ϵ_1 as the error of Hamiltonian function caused by the neural network. Hamiltonian function becomes:

$$H(s, \tau, V_s^*) = \hat{W}^T \Phi_s(f(s) + g_\tau \tau) + s^T Q s + \tau^T R \tau = \epsilon_1 \tag{36}$$

Define weight error:

$$\tilde{W} = W^* - \hat{W} \tag{37}$$

Substituting Equation 37 into Equation 31:

$$\epsilon_1 = -\tilde{W}^T \Phi_s(f(s) + g_\tau \tau) + \epsilon_H \tag{38}$$

To ensure $\epsilon_1 \rightarrow \epsilon_H$, $\hat{W} \rightarrow W$, thus minimizing $E = \epsilon_1^2/2$ is required to adjust the parameter \hat{W} . The update law for the weight \hat{W} can be:

$$\dot{\hat{W}} = \begin{cases} \hat{W}_c & \text{if } s^T(f(s) + g_\tau \tau) \leq 0 \\ \hat{W}_c + W_{RB} & \text{contrast} \end{cases} \tag{39}$$

where

$$\hat{W}_c = -\alpha_1 \frac{\hat{\sigma}}{(\hat{\sigma}^T \hat{\sigma} + 1)^2} (\hat{\sigma}^T \hat{W} + s^T Q s + \tau^T R \tau) \tag{40}$$

$$W_{RB} = \frac{1}{2} \alpha_2 \Phi_s g_\tau R^{-1} g_\tau^T s \tag{41}$$

with $\hat{\sigma} = \Phi_s(f(s) + g_\tau \tau)$, $\alpha_1 > 0$ $\alpha_2 > 0$ are update rate coefficients.

The optimal control signal is calculated:

$$\tau_0 = -\frac{1}{2} R^{-1} g_\tau^T \hat{W}^T \Phi_s \tag{42}$$

3.2. Discrete Disturbance Observer

In this subsection, the disturbance estimator is designed as Skjetne, et al. [28] to estimate the unknown disturbance τ_d .

From dynamic model (3), we have:

$$\dot{\vartheta} = -M^{-1}(C(\vartheta) + D(\vartheta))\vartheta + M^{-1}\tau + M^{-1}\tau_d \tau_0 = -\frac{1}{2} R^{-1} g_\tau^T \hat{W}^T \Phi_s \tag{43}$$

Define $A = -M^{-1}(C(\vartheta) + D(\vartheta))$, $B = M^{-1}$, $G = M^{-1}$, $d = \tau_d$. Then the dynamic equation becomes:

$$\dot{\vartheta} = A\vartheta + B\tau + Gd \tag{44}$$

Assumption 2. $rank(G) = 3 \forall \vartheta, t$

In the discrete domain, the derivative operator can be approximated by the Euler formula:

$$\vartheta_{k+1} \approx \vartheta_k + \Delta_T \dot{\vartheta}_k \tag{45}$$

with Δ_T as the sample time, ϑ_k as the velocity of the USV at time T_k .

Then, the discrete-time dynamic equation can be written:

$$\vartheta_{k+1} \approx \vartheta_k \vartheta_k \approx A_k^\vartheta \vartheta_{k-1} + B_k^\vartheta \tau_{k-1} + G_k^\vartheta d_k + \Delta_T \dot{\vartheta}_k \tag{46}$$

where $d_k = d(T_k)$, $I_3 \in \mathbb{R}^{3 \times 3}$ is the identity matrix and:

$$\begin{cases} A_k^\vartheta = I_3 + \Delta_T A(\vartheta_{k-1}, T_k) \\ B_k^\vartheta = \Delta_T B(\vartheta_{k-1}, T_k) \\ G_k^\vartheta = \Delta_T G(\vartheta_{k-1}, T_k) \end{cases} \tag{47}$$

The discrete disturbance observer is designed as the following:

$$\begin{cases} z_k = A_k^z z_{k-1} + B_k^z \tau_{k-1} \\ h_k = \vartheta_k - z_k - A_k^\vartheta \vartheta_{k-1} + A_k^z z_{k-1} \\ \hat{d}_k = ((G_k^\vartheta)^T G_k^\vartheta)^{-1} (G_k^\vartheta)^T h_k \end{cases} \tag{48}$$

where $A_k^z = I_3 + \Delta_T A(z_{k-1}, T_k)$, \hat{d} denotes the component that estimates the disturbance τ_d .

Finally, the overall control signal is modified as:

$$\tau = \tau_0 - g_\tau^{-1} g_d (F + \hat{d}) \tag{49}$$

3.3. Stability Analysis

Theorem 1. For the system described in Equation 23 if the controller is implemented as defined in Equation 49 and the update laws follow Equation 40 and Equation 41 the proposed RL-based update policies will ensure that both the weight errors and the tracking errors remain ultimately uniformly bounded.

Proof.

Choose the Lyapunov function as the following:

$$V = a_1 \tilde{W}^T \tilde{W} + a_2 s^T s + a_3 \int_t^\infty (s^T Q s + \tau_o^T R \tau_o) dt \quad (50)$$

where a_1, a_2, a_3 are positive constants.

$$\begin{aligned} \dot{V} &= -2a_1 \tilde{W}^T \dot{\tilde{W}} + 2a_2 s^T (f(s) + g_\tau (\tau_o - g_\tau^{-1} g_d (F + \hat{d})) + g_d (F + d)) \\ &\quad - a_3 (s^T Q s + \tau_o^T R \tau_o) \\ &= -2a_1 \tilde{W}^T \dot{\tilde{W}} + 2a_2 s^T (f(s) + g_\tau \tau_o) + 2a_2 s^T g_d \tilde{d} - a_3 (s^T Q s + \tau_o^T R \tau_o) \end{aligned} \quad (51)$$

with $\tilde{d} = d - \hat{d}$.

Because \tilde{d} converges to zero thanks to the disturbance observer (48) and

$$s^T Q s + \tau_o^T R \tau_o \geq \lambda_{\min}(Q) \|s\|^2 + \lambda_{\min}(R) \|\tau_o\|^2 \quad (52)$$

the following inequality is obtained:

$$\dot{V} \leq -2a_1 \tilde{W}^T \dot{\tilde{W}} + 2a_2 s^T (f(s) + g_\tau \tau_o) + a_2 \|s\|^2 - a_3 \lambda_{\min}(Q) \|s\|^2 - a_3 \lambda_{\min}(R) \|\tau_o\|^2 \quad (53)$$

Case 1. When $s^T (f(s) + g_\tau \tau_o) > 0$, then $\tilde{W} = \hat{W}_c + W_{RB}$

$$\begin{aligned} -\tilde{W}^T \dot{\tilde{W}} &= -\tilde{W}^T \left(-\alpha_1 \frac{\hat{\sigma}}{(\hat{\sigma}^T \hat{\sigma} + 1)^2} (\hat{\sigma}^T \tilde{W} + s^T Q s + \tau^T R \tau) + \frac{1}{2} \alpha_2 \Phi_s g_\tau R^{-1} g_\tau^T s \right) \\ &= -\alpha_1 \frac{\tilde{W}^T \hat{\sigma} \hat{\sigma}^T \tilde{W}}{(\hat{\sigma}^T \hat{\sigma} + 1)^2} + \alpha_1 \frac{\tilde{W}^T \hat{\sigma}}{(\hat{\sigma}^T \hat{\sigma} + 1)^2} e_H - \frac{\alpha_2}{2} \tilde{W}^T \Phi_s g_\tau R^{-1} g_\tau^T s \end{aligned} \quad (54)$$

with $e_H = \hat{\sigma}^T W^* + s^T Q s + \tau^T R \tau$.

According to Young inequality:

$$\begin{cases} 2 \frac{\tilde{W}^T \hat{\sigma}}{(\hat{\sigma}^T \hat{\sigma} + 1)^2} e_H \leq \left\| \frac{\hat{\sigma}}{\hat{\sigma}^T \hat{\sigma} + 1} \right\|^2 \|\tilde{W}\|^2 + \left\| \frac{e_H}{\hat{\sigma}^T \hat{\sigma} + 1} \right\|^2 \\ \frac{\tilde{W}^T \hat{\sigma} \hat{\sigma}^T \tilde{W}}{(\hat{\sigma}^T \hat{\sigma} + 1)^2} = \left\| \frac{\hat{\sigma}}{\hat{\sigma}^T \hat{\sigma} + 1} \right\|^2 \|\tilde{W}\|^2 \end{cases} \quad (55)$$

Therefore:

$$-\tilde{W}^T \dot{\tilde{W}} \leq -\frac{\alpha_1}{2} \left\| \frac{\hat{\sigma}}{\hat{\sigma}^T \hat{\sigma} + 1} \right\|^2 \|\tilde{W}\|^2 + \frac{\alpha_1}{2} \left\| \frac{e_H}{\hat{\sigma}^T \hat{\sigma} + 1} \right\|^2 - \frac{\alpha_2}{2} \tilde{W}^T \Phi_s g_\tau R^{-1} g_\tau^T s \quad (56)$$

Subsequently, because $f(s)$ is Lipschitz continuous, $\exists k > 0: s^T f(s) \leq k \|s\|^2$

Then

$$s^T (f(s) + g_\tau \tau_o) \leq k \|s\|^2 - \frac{1}{2} s^T g_\tau R^{-1} g_\tau^T \tilde{W}^T \Phi_s \quad (57)$$

Substituting Equations 56-57 into Equation 53:

$$\begin{aligned} \dot{V} &\leq -a_1 \alpha_1 \left\| \frac{\hat{\sigma}}{\hat{\sigma}^T \hat{\sigma} + 1} \right\|^2 \|\tilde{W}\|^2 + a_1 \alpha_1 \left\| \frac{e_H}{\hat{\sigma}^T \hat{\sigma} + 1} \right\|^2 + (2k + 1) a_2 \|s\|^2 \\ &\quad - (a_1 \alpha_2 \tilde{W}^T + a_2 \tilde{W}^T) \Phi_s g_\tau R^{-1} g_\tau^T s - a_3 \lambda_{\min}(Q) \|s\|^2 - a_3 \lambda_{\min}(R) \|\tau_o\|^2 \end{aligned} \quad (58)$$

Let $a_2 = a_1 \alpha_2$:

$$\begin{aligned} \dot{V} &\leq -a_1 \alpha_1 \left\| \frac{\hat{\sigma}}{\hat{\sigma}^T \hat{\sigma} + 1} \right\|^2 \|\tilde{W}\|^2 + a_1 \alpha_1 \left\| \frac{e_H}{\hat{\sigma}^T \hat{\sigma} + 1} \right\|^2 + (2k + 1) a_2 \|s\|^2 - a_2 \tilde{W}^T \Phi_s g_\tau R^{-1} g_\tau^T s \\ &\quad - a_3 \lambda_{\min}(Q) \|s\|^2 - a_3 \lambda_{\min}(R) \|\tau_o\|^2 \end{aligned} \quad (59)$$

Let $k_{\max} = W_{\max}^T \Phi_s \max g_\tau \max R^{-1} g_\tau^T \max$:

$$\begin{aligned} \dot{V} &\leq -a_1 \alpha_1 \left\| \frac{\hat{\sigma}}{\hat{\sigma}^T \hat{\sigma} + 1} \right\|^2 \|\tilde{W}\|^2 + a_1 \alpha_1 \left\| \frac{e_H}{\hat{\sigma}^T \hat{\sigma} + 1} \right\|^2 + (2k + 1) a_2 \|s\|^2 - a_3 \lambda_{\min}(Q) \|s\|^2 \\ &\quad - a_3 \lambda_{\min}(R) \|\tau_o\|^2 + \frac{a_2 k_{\max}^2}{2} + \frac{a_2}{2} \|s\|^2 \end{aligned} \quad (60)$$

Let

$$\begin{aligned} a_{w1} &= -a_1 \alpha_1 \left\| \frac{\hat{\sigma}}{\hat{\sigma}^T \hat{\sigma} + 1} \right\|^2, a_{s1} = \left(2k + \frac{3}{2} \right) a_2 - a_3 \lambda_{\min}(Q), \\ a_{\tau1} &= -a_3 \lambda_{\min}(R), a_{e1} = a_1 \alpha_1 \left\| \frac{e_H}{\hat{\sigma}^T \hat{\sigma} + 1} \right\|^2 + \frac{a_2 k_{\max}^2}{2} \end{aligned}$$

Equation 60 can be rewritten:

$$\dot{V} \leq a_{w1} \|\tilde{W}\|^2 + a_{s1} \|s\|^2 + a_{\tau1} \|\tau_o\|^2 + a_{e1} \quad (61)$$

Let $X = [\tilde{W}; s; \tau_o]$, we have:

$$\dot{V} \leq a_{X1} \|X\|^2 \quad (62)$$

if the following conditions are satisfied:

$$\begin{cases} a_3 \geq \frac{4k+3}{2\lambda_{\min}(Q)} a_2, a_2 = a_1 \alpha_2 \\ \|\tilde{W}\|^2 \geq \sqrt{\frac{a_{e1}}{-a_{w1}}}, \|s\|^2 \geq \sqrt{\frac{a_{e1}}{-a_{s1}}}, \|\tau_o\|^2 \geq \sqrt{\frac{a_{e1}}{-a_{\tau1}}} \end{cases} \quad (63)$$

with $a_{x1} \leq \max\{a_{w1}, a_{s1}, a_{\tau1}\} < 0$

Case 2. When $f(s) + g_\tau \tau_o \leq 0$, then $\dot{\hat{W}} = \dot{\hat{W}}_c$

From Equation 56, we have

$$-\tilde{W}^T \dot{\hat{W}} \leq -\frac{\alpha_1}{2} \left\| \frac{\hat{\sigma}}{\hat{\sigma}^T \hat{\sigma} + 1} \right\|^2 \|\tilde{W}\|^2 + \frac{\alpha_1}{2} \left\| \frac{e_H}{\hat{\sigma}^T \hat{\sigma} + 1} \right\|^2 \quad (64)$$

Since $s^T(f(s) + g_\tau \tau_o) \leq 0$, there exists $k_s > 0$ that $s^T(f(s) + g_\tau \tau_o) \leq -k_s \|s\|^2$

Therefore

$$\begin{aligned} \dot{V} \leq & -a_1 \alpha_1 \left\| \frac{\hat{\sigma}}{\hat{\sigma}^T \hat{\sigma} + 1} \right\|^2 \|\tilde{W}\|^2 + a_1 \alpha_1 \left\| \frac{e_H}{\hat{\sigma}^T \hat{\sigma} + 1} \right\|^2 - a_3 \lambda_{\min}(R) \|\tau_o\|^2 \\ & + (a_2 - 2a_2 k_s - a_3 \lambda_{\min}(Q)) \|s\|^2 \end{aligned} \quad (65)$$

Choose $a_{w2} = -a_1 \alpha_1 \left\| \frac{\hat{\sigma}}{\hat{\sigma}^T \hat{\sigma} + 1} \right\|^2$, $a_{s2} = (a_2 - 2a_2 k_s - a_3 \lambda_{\min}(Q))$, $a_{\tau2} = -a_3 \lambda_{\min}(R)$, $a_{e2} = a_1 \alpha_1 \left\| \frac{e_H}{\hat{\sigma}^T \hat{\sigma} + 1} \right\|^2$. Eq.

(65) can be rewritten:

$$\dot{V} \leq a_{w2} \|\tilde{W}\|^2 + a_{s2} \|s\|^2 + a_{\tau2} \|\tau_o\|^2 + a_{e2} \quad (66)$$

If

$$\begin{cases} a_3 \geq \frac{a_2 - 2a_2 k_s}{\lambda_{\min}(Q)} a_2, a_2 = a_1 \alpha_2 \\ \|\tilde{W}\|^2 \geq \sqrt{\frac{a_{e2}}{-a_{w2}}}, \|s\|^2 \geq \sqrt{\frac{a_{e2}}{-a_{s2}}}, \|\tau_o\|^2 \geq \sqrt{\frac{a_{e2}}{-a_{\tau2}}} \end{cases} \quad (67)$$

Then

$$\dot{V} \leq a_{x2} \|X\|^2 \quad (68)$$

with $a_{x2} \leq \max\{a_{w2}, a_{s2}, a_{\tau2}\} < 0$.

According Equation 63 and Equation 68 the closed-loop system is UUB.

4. Simulation Result

In this section, the comparison among the proposed controller (OADP), the online actor-critic algorithm-based controller (AC), and the sliding mode controller (SMC) will be carried out.

In the first scenario, the USV will track the desired trajectory without external and unknown disturbances to compare the cost functions of the controllers. In the second one, the external and unknown disturbances will be provided to show the advantages of the disturbance estimator.

The reference trajectory of the USV is provided as follows:

$$\begin{cases} x_d = 2 \sin(0.1t) \\ y_d = 1.5 - 1.5 \cos(0.1t) \\ \psi_d = 0.02t \end{cases}$$

The USV's parameters are set as same as Skjetne, et al. [28] in Table 1.

Table 1.

USV's parameters.

Parameters	Value	Parameters	Value
m (kg)	23.8	Y_v	-0.8612
I_z (kg.m ²)	1.76	Y_{vv}	-36.2823
x_g (m)	0.046	Y_{rv}	-8.05
$X_{\dot{u}}$	-2.0	Y_r	0.1079
$Y_{\dot{v}}$	-10.0	Y_{vr}	-0.845
$Y_{\dot{r}}$	0	Y_{rr}	-3.45
$N_{\dot{v}}$	0	N_v	0.1052
$N_{\dot{r}}$	-1	N_{vv}	5.0437
X_u	-0.7225	N_{rv}	0.13
X_{uu}	-1.3274	N_r	-1.9
X_{uuu}	-5.8664	N_{vr}	0.08
N_{rr}	-0.75		

The matrices for the performance index $J = \frac{1}{2} \int_0^\infty e^T Q e + \tau^T R \tau$ are $Q = I_3$, $R = I_3$. The activation function of the proposed controller is chosen as $\Phi(s) = [s_1^2, s_2^2, s_3^2]^T$. The estimated weight vector is initialized as $\hat{W} = [300 \ 300 \ 30]^T$.

The actor-critic algorithm is designed as Vamvoudakis and Lewis [12]. The activation vector and control parameters of the actor – critic algorithm are initialized as: $\sigma = [s_1^2, s_2^2, s_3^2, s_1 s_2, s_2 s_3, s_3 s_1]^T$, $W_a = W_c = [1, 1, 1, 1, 1, 1]^T$

The control input of the sliding mode controller is implemented as Cheng, et al. [29]: $W = \text{diag}([0.2, 0.2, 0.1])$, $W = \text{diag}([0.1, 0.1, 0.1])$.

Moreover, the maximum values of the control inputs are set as $\tau_{1\max} = \tau_{2\max} = 20N$, $\tau_{3\max} = 10 Nm$.

Case 1: Simulation in the environment without disturbances

The trajectory of the USV is shown in the Figure 2 with each controller. The results show that the proposed controller tracks the reference trajectory more quickly and accurately than the other controllers.

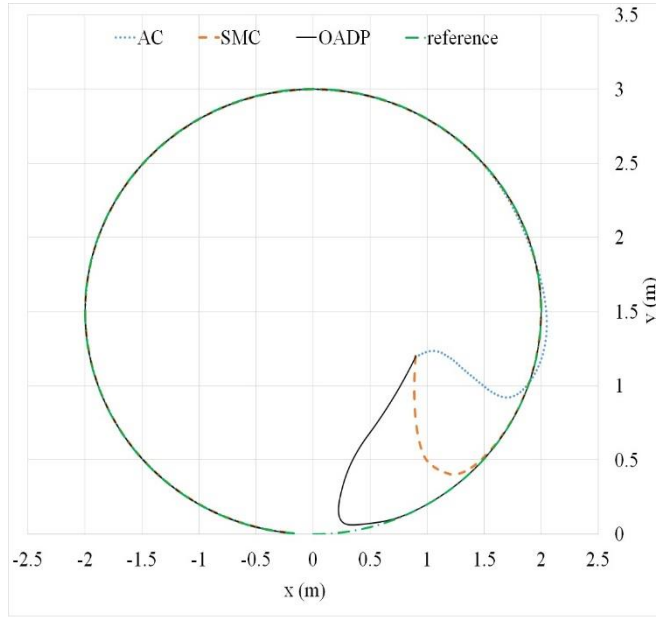


Figure 2.
Circle trajectory without unknown disturbance.

The plot of trajectory errors is shown in Figure 3 that the proposed controller reduces the tracking error to nearly zero within approximately three seconds while the SMC takes 8s and the AC controller takes approximately 18s.

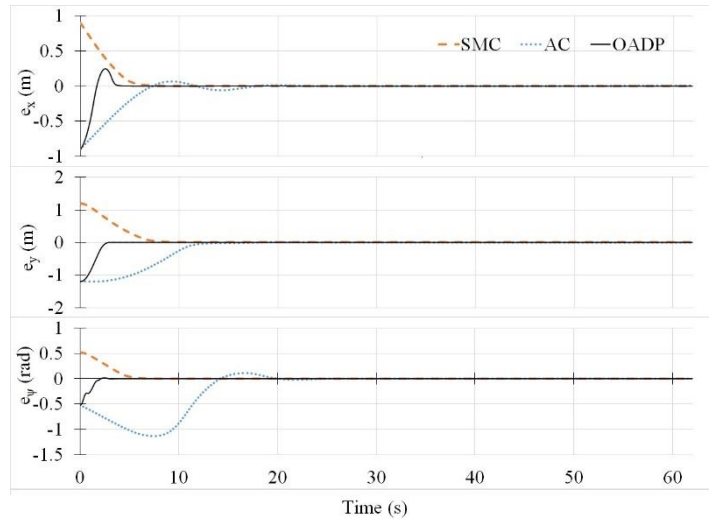


Figure 3.
Circle trajectory errors without unknown disturbance.

The control inputs $\tau = [\tau_1, \tau_2, \tau_3]^T$ of each controller are presented in the Figure 4. The proposed controller provides a smoother and more effective control signal, making it suitable for actuator operation. In contrast, the online AC algorithm-based controller exhibits high-frequency oscillations during the first second, while the SMC controller suffers from chattering throughout the control process, which makes them less suitable for actuator implementation.

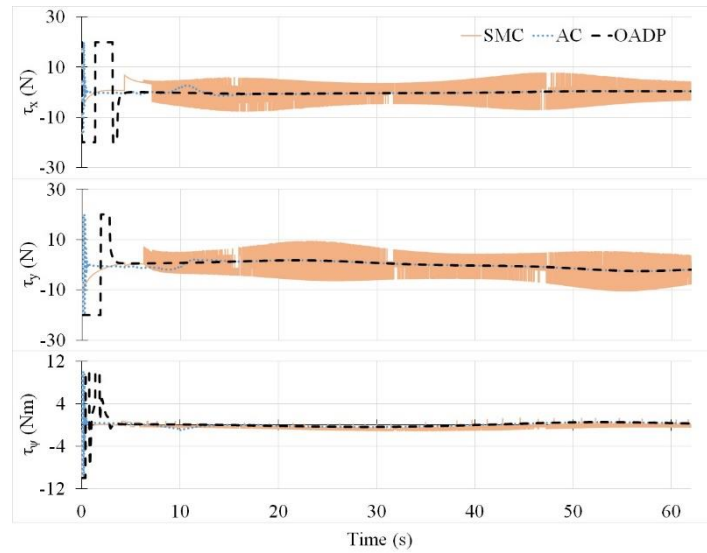


Figure 4.
Control signals without unknown disturbance.

Figure 5 shows that the proposed controller is the most cost-effective, requiring only 6.25% of the cost compared to the SMC.

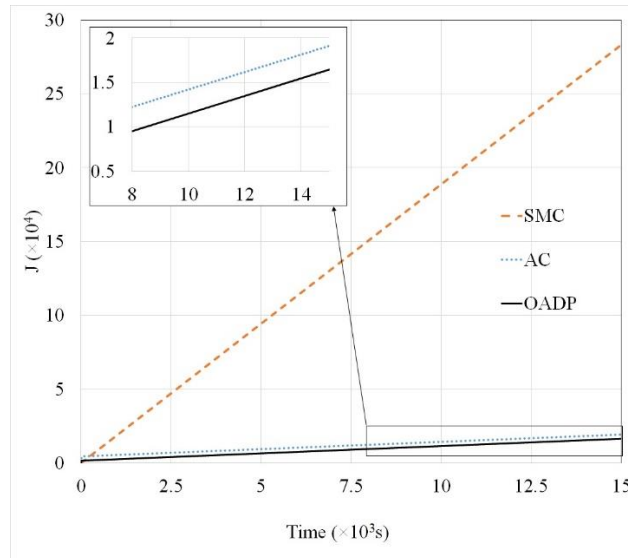


Figure 5.
Performance index.

The estimated weights of proposed controller are shown in Figure 6. The neural network weights converge to their optimal values after around 3 seconds.

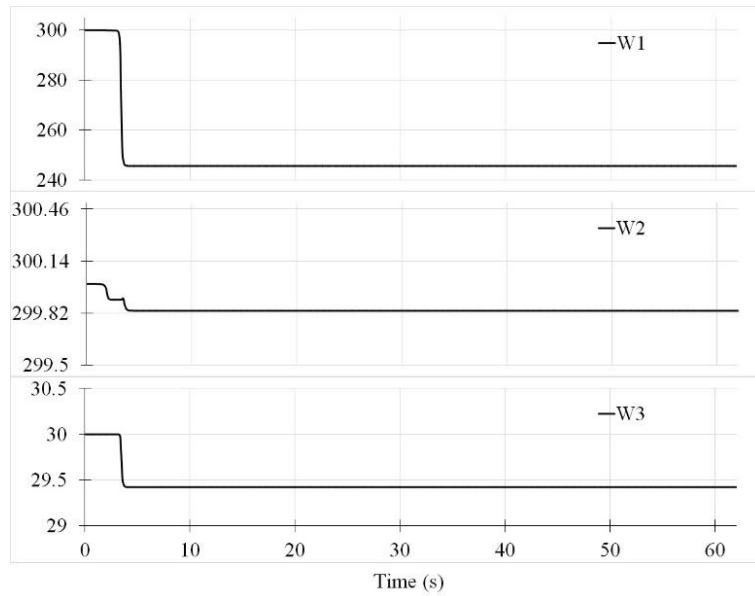


Figure 6.
Estimated weights.

Case 2: Simulation in the case of the external and unknown disturbances

The disturbances are provided as:

$$\begin{cases} d_x = 2.6 + 4 \sin(0.02t) + 3 \sin(0.1t) \\ d_y = -1.8 + 4 \sin\left(0.02t - \frac{\pi}{6}\right) + 3 \sin(0.3t) \\ d_\psi = -2 \sin(0.09t + \pi/3) - 8 \sin(0.01t) \end{cases}$$

The disturbances estimation is shown in the Figure 7. The proposed disturbance observer tracks the disturbance after five seconds.

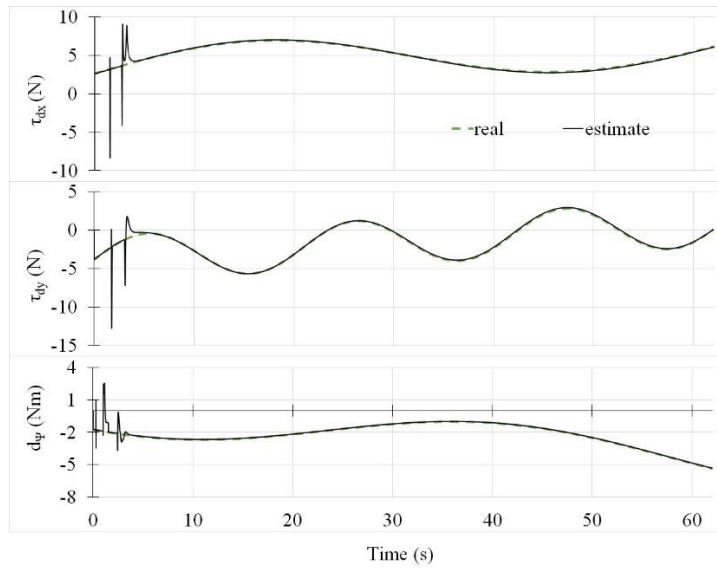


Figure 7.
Disturbance estimation.

The trajectory of the USV with external and unknown disturbances is shown in Figure 8. By effectively estimating disturbances, the proposed controller accurately tracks the reference trajectory, whereas the SMC controller exhibits significant errors and fails to follow the trajectory. The AC controller follows the reference trajectory in the first half of the cycle, but under the influence of unknown disturbances, the tracking error increases quite significantly in the last half of the cycle.

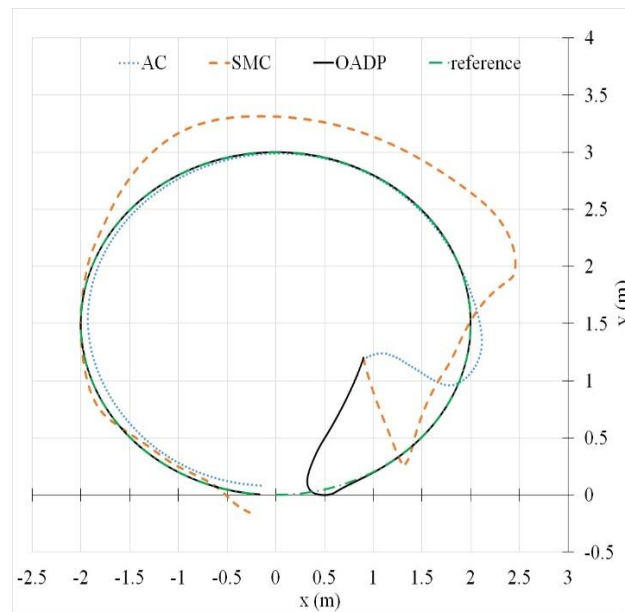


Figure 8.
Circle trajectory.

5. Conclusions

In this paper, the trajectory tracking problem under external unknown disturbances is addressed by employing the Online Adaptive Dynamic Programming (OADP) algorithm and integrating a discrete disturbance observer.

The simulation results demonstrate that the proposed control system achieves improved energy optimization and trajectory tracking performance in comparison with sliding mode controller and online actor-critic algorithm-based controller.

The proposed controller sufficiently eliminates the chattering phenomenon associated with sliding mode control while significantly reducing computation time therefore improving the performance compared to the online actor-critic algorithm approach.

Future research will focus on extending the proposed method to control the multi-USV systems.

References

- [1] Z. Liu, Y. Zhang, X. Yu, and C. Yuan, "Unmanned surface vehicles: An overview of developments and challenges," *Annual Reviews in Control*, vol. 41, pp. 71-93, 2016. <https://doi.org/10.1016/j.arcontrol.2016.04.018>
- [2] R.-j. Yan, S. Pang, H.-b. Sun, and Y.-j. Pang, "Development and missions of unmanned surface vehicle," *Journal of Marine Science and Application*, vol. 9, no. 4, pp. 451-457, 2010. <https://doi.org/10.1007/s11804-010-1033-2>
- [3] L. McLauchlan, "Simulation and control of an unmanned surface vehicle," in *Proc. ASEE Annual Conference & Exposition, Indianapolis, Indiana, USA*, 2014.
- [4] Y.-H. Chen, M.-Z. Ellis-Tiew, Y.-H. Chan, G.-W. Lin, and Y.-Y. Chen, "Trajectory tracking design for unmanned surface vessels: Robust control approach," *Journal of Marine Science and Engineering*, vol. 11, no. 8, p. 1612, 2023. <https://doi.org/10.3390/jmse11081612>
- [5] Z.-P. Jiang, "Global tracking control of underactuated ships by Lyapunov's direct method," *Automatica*, vol. 38, no. 2, pp. 301-309, 2002. [https://doi.org/10.1016/S0005-1098\(01\)00199-6](https://doi.org/10.1016/S0005-1098(01)00199-6)
- [6] K. Y. Pettersen and H. Nijmeijer, "Underactuated ship tracking control: Theory and experiments," *International Journal of Control*, vol. 74, no. 14, pp. 1435-1446, 2001. <https://doi.org/10.1080/00207170110072039>
- [7] K. D. Do, Z.-P. Jiang, and J. Pan, "Underactuated ship global tracking under relaxed conditions," *IEEE Transactions on Automatic Control*, vol. 47, no. 9, pp. 1529-1536, 2002. <https://doi.org/10.1109/TAC.2002.802755>
- [8] K. D. Do, Z. P. Jiang, J. Pan, and H. Nijmeijer, "A global output-feedback controller for stabilization and tracking of underactuated ODIN: A spherical underwater vehicle," *Automatica*, vol. 40, no. 1, pp. 117-124, 2004. <https://doi.org/10.1016/j.automatica.2003.08.004>
- [9] R. Yu, Q. Zhu, G. Xia, and Z. Liu, "Sliding mode tracking control of an underactuated surface vessel," *IET Control Theory & Applications*, vol. 6, no. 3, pp. 461-466, 2012.
- [10] C. Shen, Y. Shi, and B. Buckham, "Trajectory tracking control of an autonomous underwater vehicle using Lyapunov-based model predictive control," *IEEE Transactions on Industrial Electronics*, vol. 65, no. 7, pp. 5796-5805, 2017. <https://doi.org/10.1109/TIE.2017.2779442>
- [11] R. Bellman, "Dynamic Programming," *science*, vol. 153, no. 3731, pp. 34-37, 1966.
- [12] K. G. Vamvoudakis and F. L. Lewis, "Online actor-critic algorithm to solve the continuous-time infinite horizon optimal control problem," *Automatica*, vol. 46, no. 5, pp. 878-888, 2010. <https://doi.org/10.1016/j.automatica.2010.02.018>
- [13] A. Falsone, L. Deori, D. Ioli, S. Garatti, and M. Prandini, "Optimal disturbance compensation for constrained linear systems operating in stationary conditions: A scenario-based approach," *Automatica*, vol. 110, p. 108537, 2019. <https://doi.org/10.1016/j.automatica.2019.108537>
- [14] A. Mohammadi, M. Tavakoli, and H. Marquez, "Disturbance observer-based control of non-linear haptic teleoperation systems," *IET Control Theory & Applications*, vol. 5, no. 18, pp. 2063-2074, 2011. <https://doi.org/10.1049/iet-cta.2010.0517>

- [15] C. Du, H. Li, C. Thum, F. Lewis, and Y. Wang, "Simple disturbance observer for disturbance compensation," *IET Control Theory & Applications*, vol. 4, no. 9, pp. 1748-1755, 2010. <https://doi.org/10.1049/iet-cta.2009.0178>
- [16] F. Castanos and L. Fridman, "Analysis and design of integral sliding manifolds for systems with unmatched perturbations," *IEEE Transactions on Automatic Control*, vol. 51, no. 5, pp. 853-858, 2006. <https://doi.org/10.1109/TAC.2006.875008>
- [17] M. Rubagotti, A. Estrada, F. Castaños, A. Ferrara, and L. Fridman, "Integral sliding mode control for nonlinear systems with matched and unmatched perturbations," *IEEE Transactions on Automatic Control*, vol. 56, no. 11, pp. 2699-2704, 2011. <https://doi.org/10.1109/TAC.2011.2159420>
- [18] N. N. Nam, N.-D. Nguyen, and Y. I. Lee, "Model predictive control for a voltage sensorless grid-connected inverter with LCL filter using lumped disturbance observer," *IEEE Journal of Emerging and Selected Topics in Power Electronics*, vol. 11, no. 3, pp. 3050-3063, 2023.
- [19] J.-H. She, M. Fang, Y. Ohyama, H. Hashimoto, and M. Wu, "Improving disturbance-rejection performance based on an equivalent-input-disturbance approach," *IEEE Transactions on Industrial Electronics*, vol. 55, no. 1, pp. 380-389, 2008. <https://doi.org/10.1109/TIE.2007.905976>
- [20] Y. Xiong and M. Saif, "Unknown disturbance inputs estimation based on a state functional observer design," *Automatica*, vol. 39, no. 8, pp. 1389-1398, 2003. [https://doi.org/10.1016/S0005-1098\(03\)00087-6](https://doi.org/10.1016/S0005-1098(03)00087-6)
- [21] J. Zhang and F. Zhu, "Output control of MIMO system with unmatched disturbance based on high-order unknown input observer," *International Journal of Control, Automation and Systems*, vol. 15, no. 2, pp. 575-584, 2017. <https://doi.org/10.1007/s12555-015-0429-9>
- [22] G. Mohamed, A. A. Sofiane, and L. Nicolas, "Adaptive super twisting extended state observer based sliding mode control for diesel engine air path subject to matched and unmatched disturbance," *Mathematics and Computers in Simulation*, vol. 151, pp. 111-130, 2018. <https://doi.org/10.1016/j.matcom.2018.03.004>
- [23] J. Yang, W.-H. Chen, and S. Li, "Autopilot design of bank-to-turn missiles using state-space disturbance observers," in *UKACC International Conference on Control 2010*, 2010: IET, pp. 1218-1223.
- [24] W.-H. Chen, D. J. Ballance, P. J. Gawthrop, and J. O'Reilly, "A nonlinear disturbance observer for robotic manipulators," *IEEE Transactions on Industrial Electronics*, vol. 47, no. 4, pp. 932-938, 2000. <https://doi.org/10.1109/41.857974>
- [25] N. H. Trinh, N. T.-T. Vu, and P. D. Nguyen, "Robust optimal tracking control using disturbance observer for robotic arm systems," *Journal of Control, Automation and Electrical Systems*, vol. 32, no. 6, pp. 1473-1484, 2021. <https://doi.org/10.1007/s40313-021-00765-2>
- [26] Z. Guo, J. Guo, X. Wang, J. Chang, and H. Huang, "Sliding mode control for systems subjected to unmatched disturbances/unknown control direction and its application," *International Journal of Robust and Nonlinear Control*, vol. 31, no. 4, pp. 1303-1323, 2021. <https://doi.org/10.1002/rnc.5336>
- [27] R. Skjetne, Ø. Smogeli, and T. I. Fossen, "Modeling, identification, and adaptive maneuvering of CyberShip II: A complete design with experiments," *IFAC Proceedings Volumes*, vol. 37, no. 10, pp. 203-208, 2004. [https://doi.org/10.1016/S1474-6670\(17\)31732-9](https://doi.org/10.1016/S1474-6670(17)31732-9)
- [28] R. Skjetne, T. I. Fossen, and P. V. Kokotović, "Adaptive maneuvering, with experiments, for a model ship in a marine control laboratory," *Automatica*, vol. 41, no. 2, pp. 289-298, 2005. <https://doi.org/10.1016/j.automatica.2004.10.006>
- [29] J. Cheng, J. Yi, and D. Zhao, "Design of a sliding mode controller for trajectory tracking problem of marine vessels," *IET Control Theory & Applications*, vol. 1, no. 1, pp. 233-237, 2007. <https://doi.org/10.1049/iet-cta:20050357>